Supplementary Data

Metal Ion as Both a Cofactor and a Probe of Metal-binding Sites in a Uranyl-Specific DNAzyme: Uranyl Photocleavage and Phosphorothioate Substitution Studies

Marjorie Cepeda-Plaza, Eric L. Null, and Yi Lu*
The authors wish it to be known that, in their opinion, the first two authors should be regarded as joint First Authors
Department of Chemistry, University of Illinois at Urbana-Champaign, Urbana, IL 61801 (USA)
* To whom correspondence should be addressed. Tel: 1-217- 333-2619; Fax: 1-217-333-2685; Email: yi-lu@illinois.edu

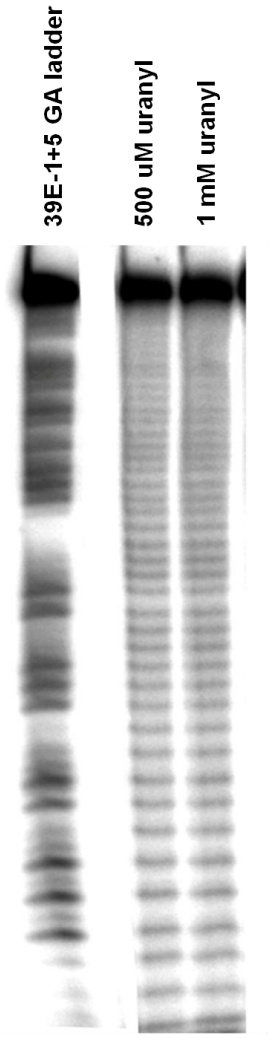

Figure S1. Gel image of uranyl photocleavage reactions of 39E (-1, +5) DNAzyme construct in the presence of 500 μM and 1 mM uranyl.

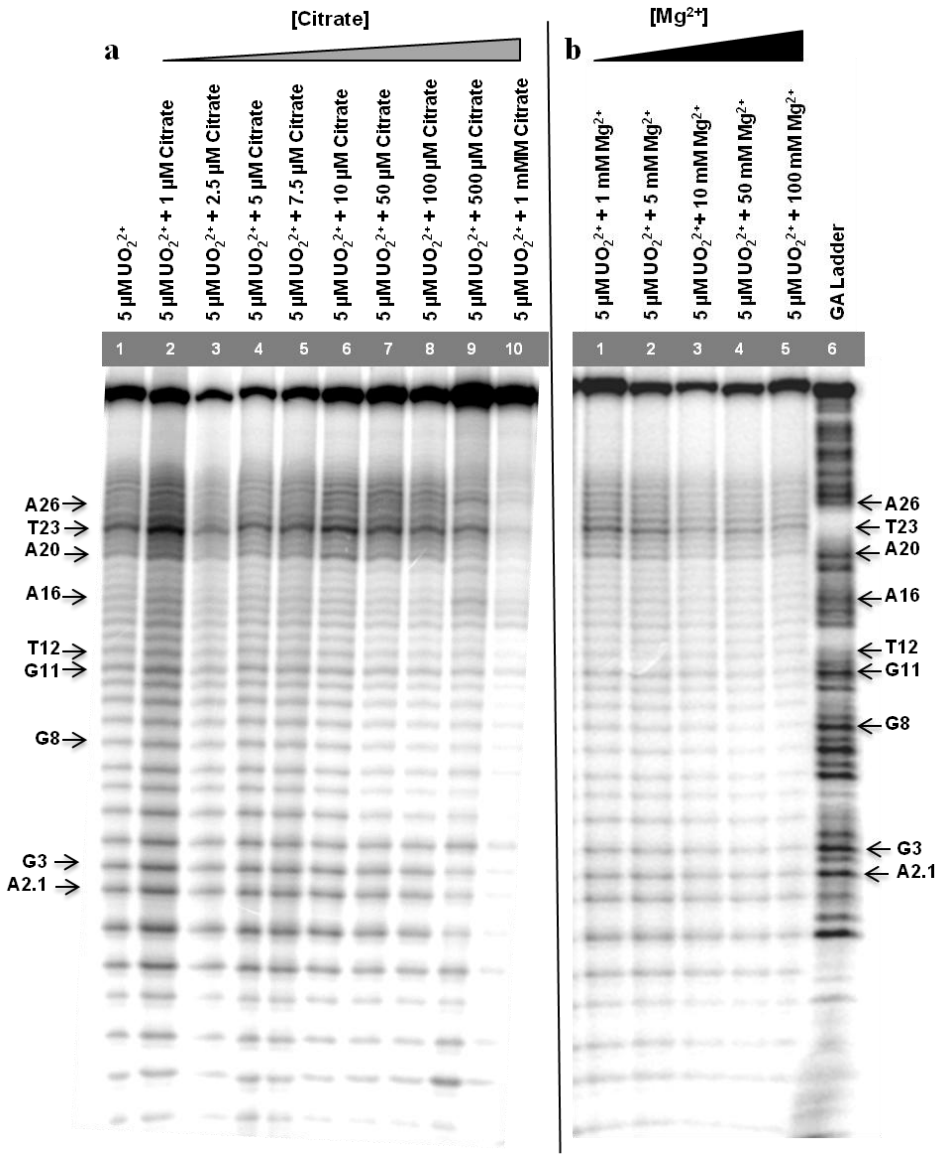

Figure S2. Gel images of uranyl photocleavage reactions of 39E (-1, +5) DNAzyme construct. (a) Photocleavage with varying concentrations of sodium citrate in the presence of 5 μM uranyl. (b) Photocleavage with varying concentrations of Mg^{2+} in the presence of 5 μM uranyl. (a) and (b) correspond to images from the same gel. Two irrelevant intervening lanes were cropped out from the image, the rest were reassembled. Dividing lanes indicate the position for this deletion.

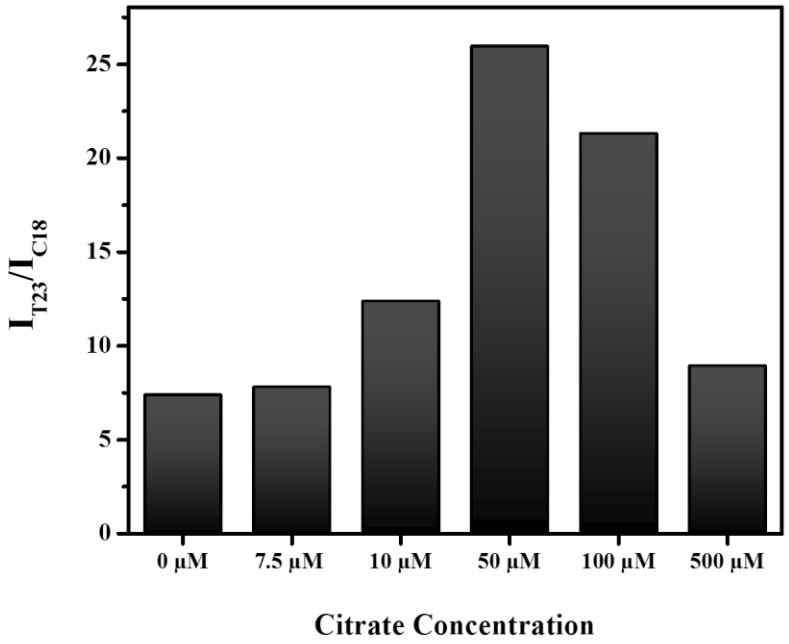

Figure S3. Ratio of the normalized cleavage intensity of the bands T23 in the bulge loop and C18 in the stem loop in presence of different concentrations of citrate.

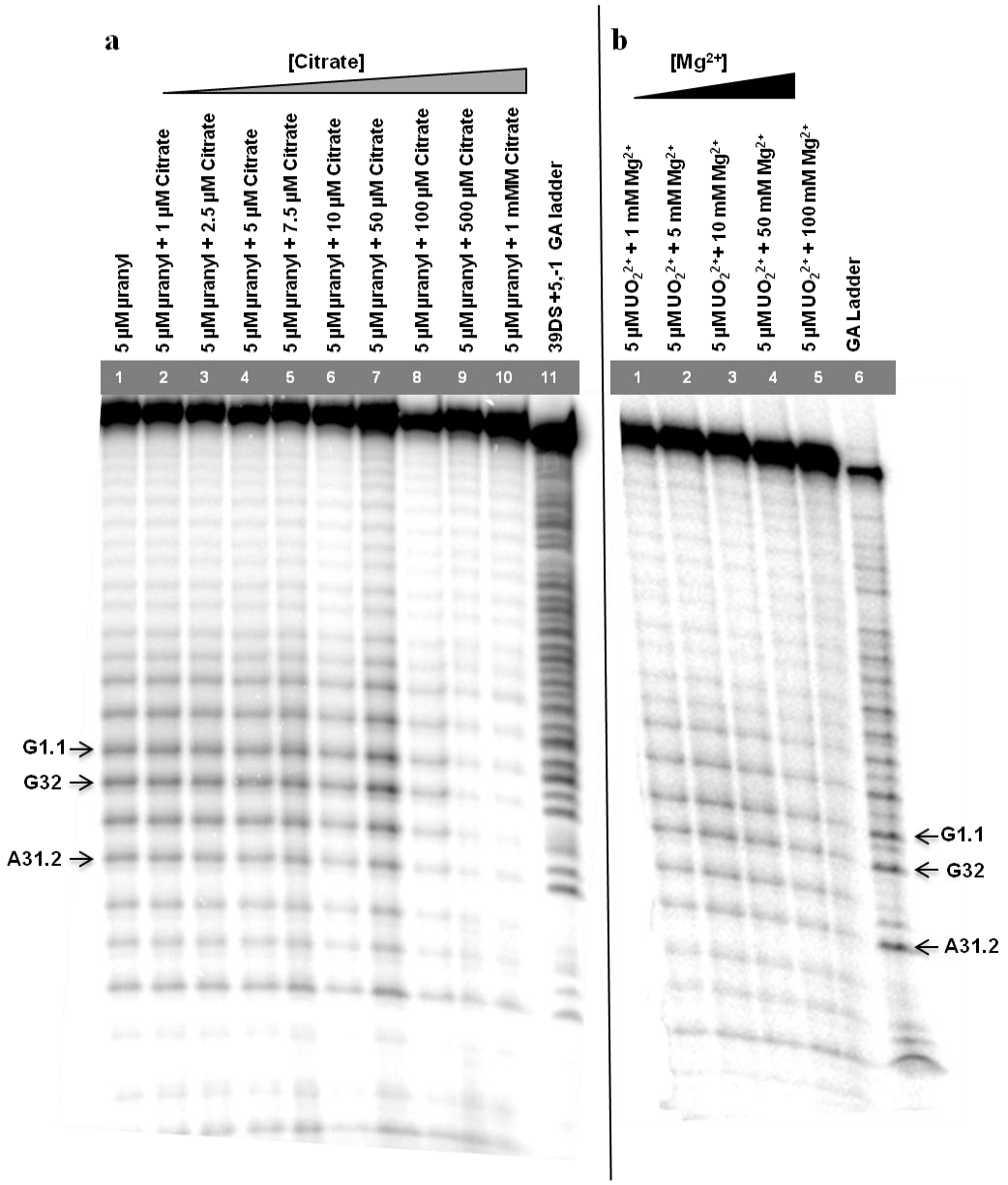

Figure S4. Gel image of uranyl photocleavage of 39DS (+5,-1). (a) Photocleavage with varying concentrations of sodium citrate. (b) Photocleavage with varying concentrations of Mg^{2+}. (a) and (b) correspond to images from the same gel. Two irrelevant intervening lanes were cropped out from the image, the rest were reassembled. Dividing lanes indicate the position for this deletion.

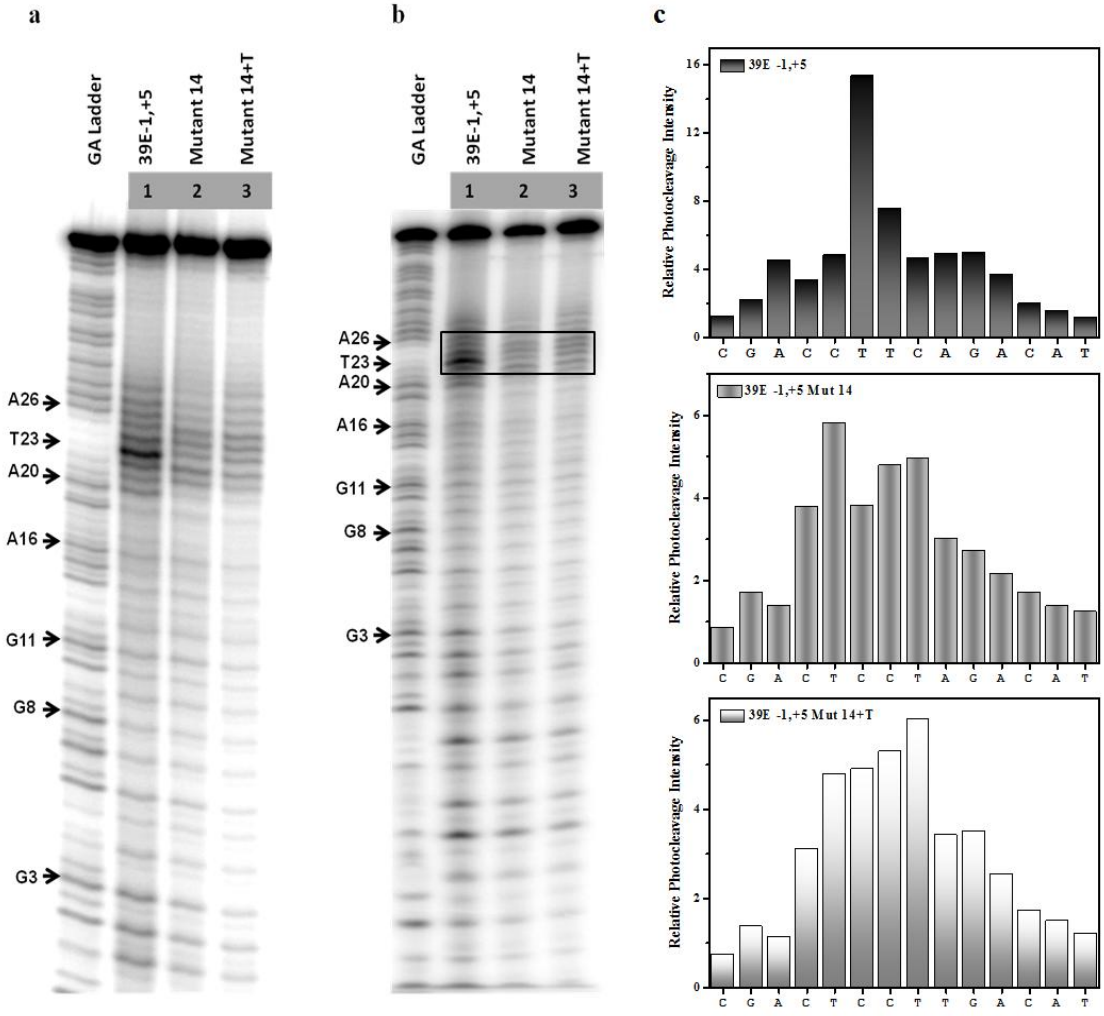

Figure S5. (a) Gel images of uranyl photocleavage reactions of 39E (-1, +5) DNAzyme construct and the variants Mutant 14 and Mutant 14+T in presence of 5 µM uranyl, run for longer time to improve resolution of the mutated region. (b) Gel images of uranyl photocleavage reactions of 39E (-1, +5) DNAzyme construct and the variants Mutant 14 and Mutant 14+T in the presence of 5 µM uranyl, run for a shorter time than (a). (c) Gel image quantification by SAFA, x-axis indicates the bands from C18-T31 according to Figure 1b. Uranyl-mediated photocleavage of the 39E DNAzyme (black), Mutant 14 (grey), and Mutant 14+T (white).

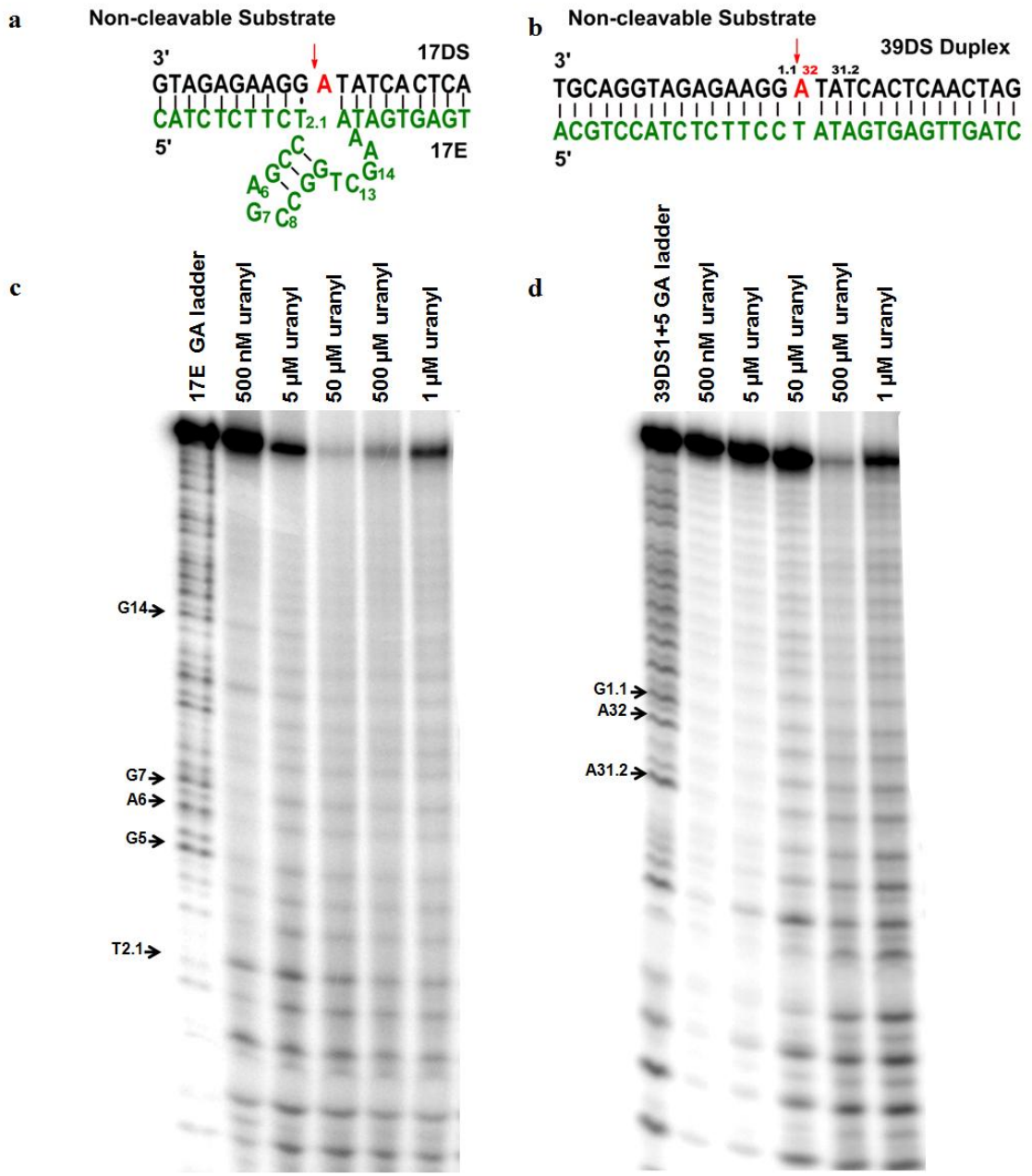

Figure S6. (a) Schematic representation of the predicted secondary structure of the trans-cleaving 8-17 DNAzyme, consisting of a DNAzyme strand (in green) and a substrate strand (in black). The substrate strand contains a single riboadenosine at the cleavage site. For the uranyl-mediated photocleavage experiments, the scissile riboadenosine was changed to deoxyriboadenosine to prevent DNAzyme-based cleavage (in red). (b) Schematic representation of the predicted secondary structure of the 39DS duplex, which consists of a substrate strand (in black) and a fully complimentary DNA strand (in green). (c) Gel image of uranyl photocleavage reactions of the 8-17 DNAzyme with varying concentrations of uranyl. (d) Gel image of uranyl photocleavage reactions of the 39DS duplex with varying concentrations of uranyl.

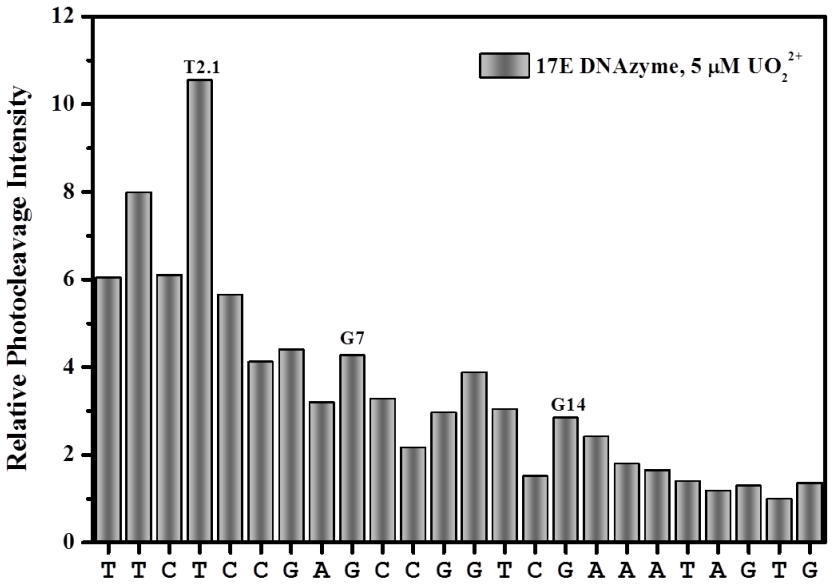

Figure S7. Uranyl photocleavage of 17E DNAzyme with the enzyme strand labeled with 5 μm uranyl. Relative photocleavage intensity obtained by gel image quantification with SAFA is plotted vs the sequence (as shown in Figure S5-a) from T2.4 to T16.6.